

The Structure of Real and Virtual Photons as measured at HERA

H. Rick

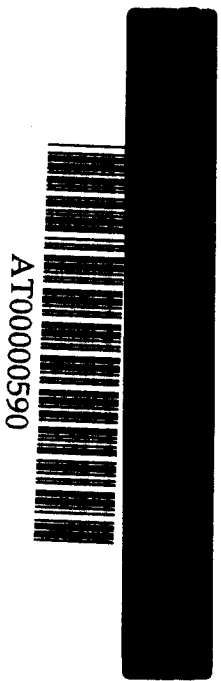
CERN-EP seminar 19/10/98

The real photon

- * kinematics
- * jet cross sections
- * parton densities
- * uncertainties

Virtual photons

- * jet cross sections
- * parton densities



CERN

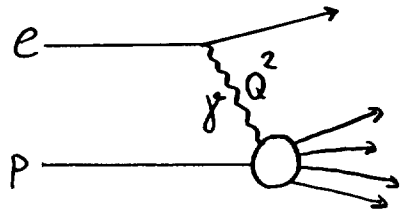
EP Monday Seminars
19 Oct 1998

294611

Contact: F. GIANNOTTI
Tel. 78965

Photoproduction of jets

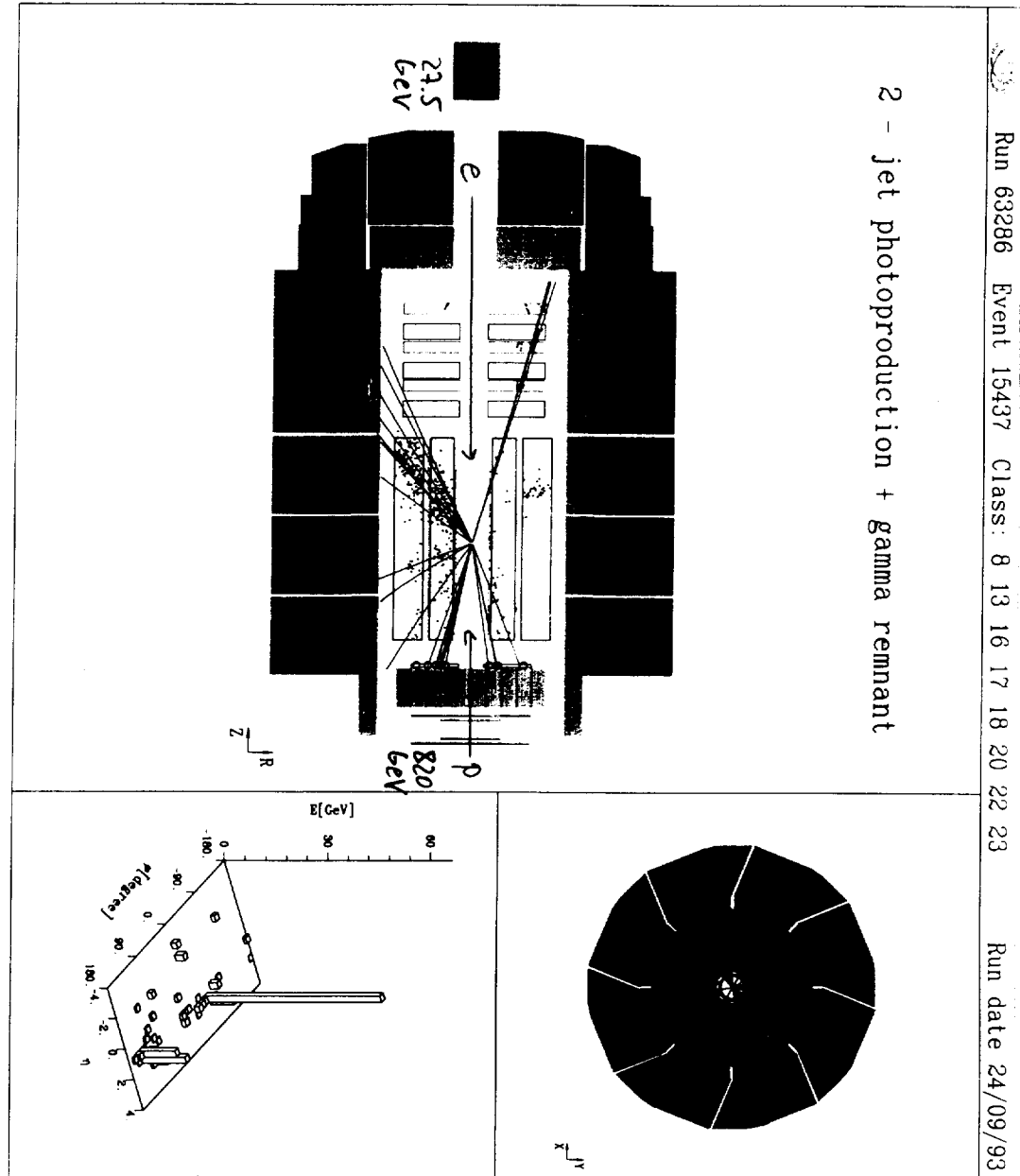
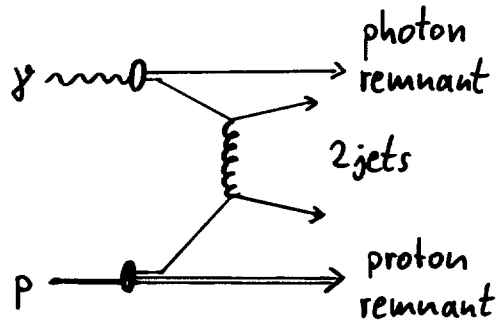
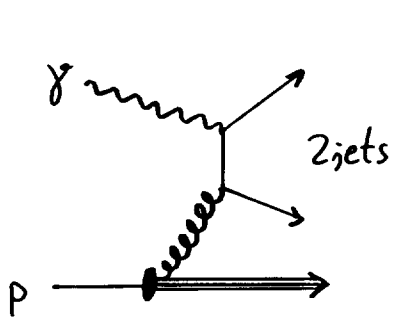
Electron-Proton scattering at HERA



$Q^2 \approx 0$ (real photon): "Photoproduction"

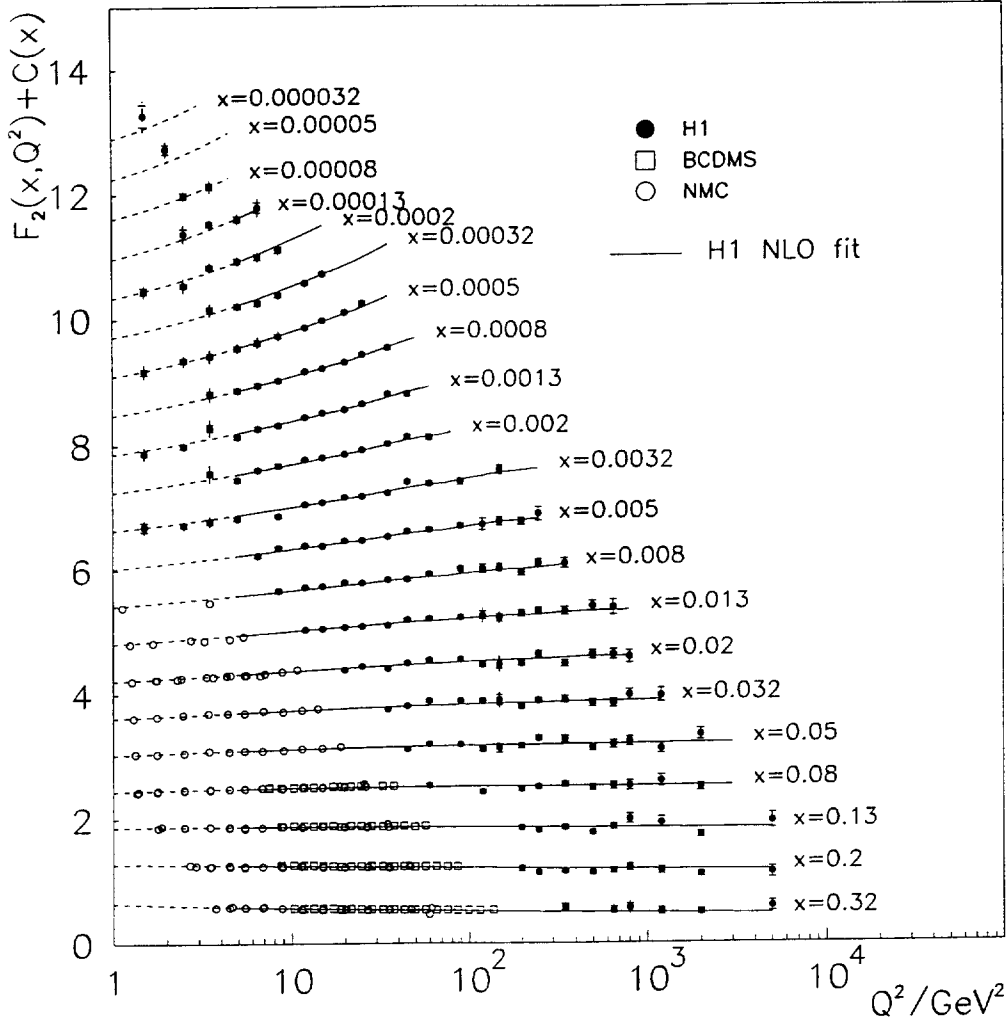
direct photon
(pointlike)

resolved photon
(with hadronic structure)



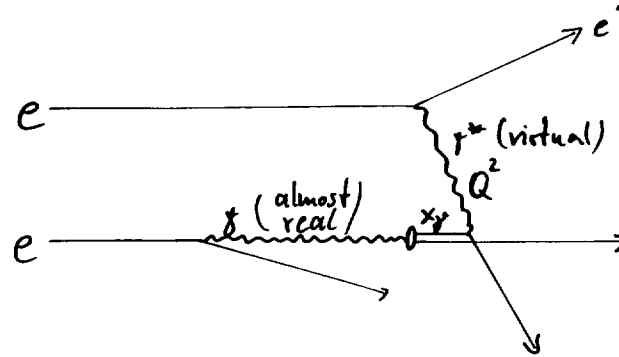
The proton structure function $F_2(x, Q^2)$

$$F_2^p \sim x \sum_q e_q^2 q^p$$



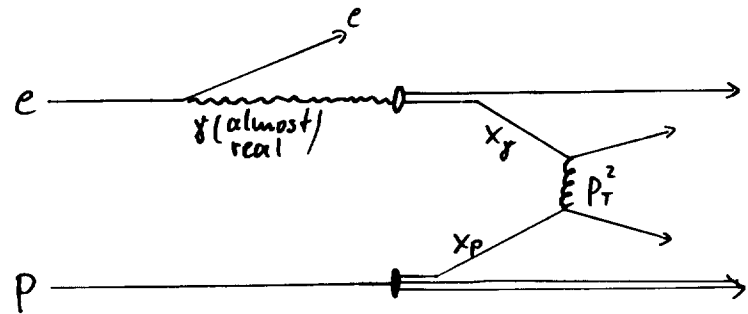
Measuring photon parton distributions

a) deep inelastic scattering at e^+e^- experiments



$$F_2^{\gamma}(x_f, Q^2) = x_f \sum_q e_q^2 (q(x_f, Q^2) + \bar{q}(x_f, Q^2))$$

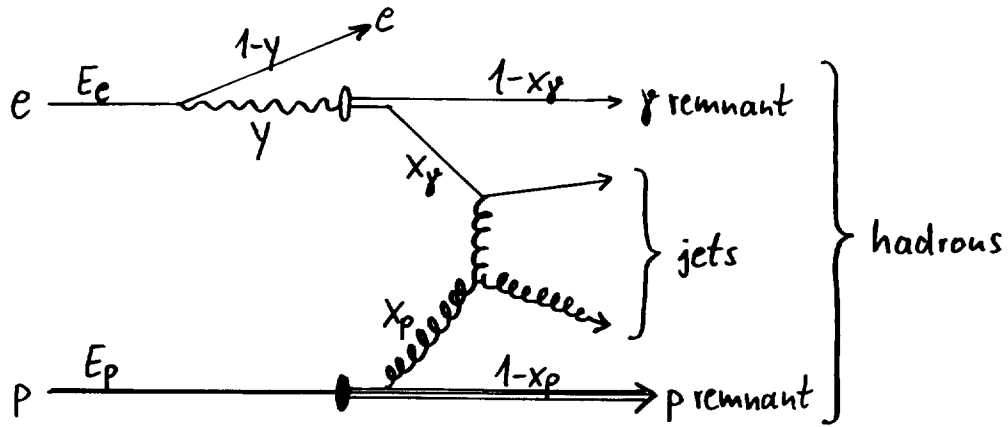
b) photoproduction at HERA (ep collisions)



hadronic scattering, both quark and gluon content of the photon contribute:

$$f_{\text{eff}}^{\gamma}(x_f, P_T^2) = \sum_q (q(x_f, P_T^2) + \bar{q}(x_f, P_T^2)) + \frac{9}{4} g(x_f, P_T^2)$$

The di-jet cross section



4 independent kinematic variables, e.g.:

$$y = \frac{E_y}{E_e} = \frac{1}{2E_e} \sum_{\text{hadrons}} (E - p_z) \quad x_y = \frac{1}{2E_y} \sum_{\text{jets}} (E - p_z)$$

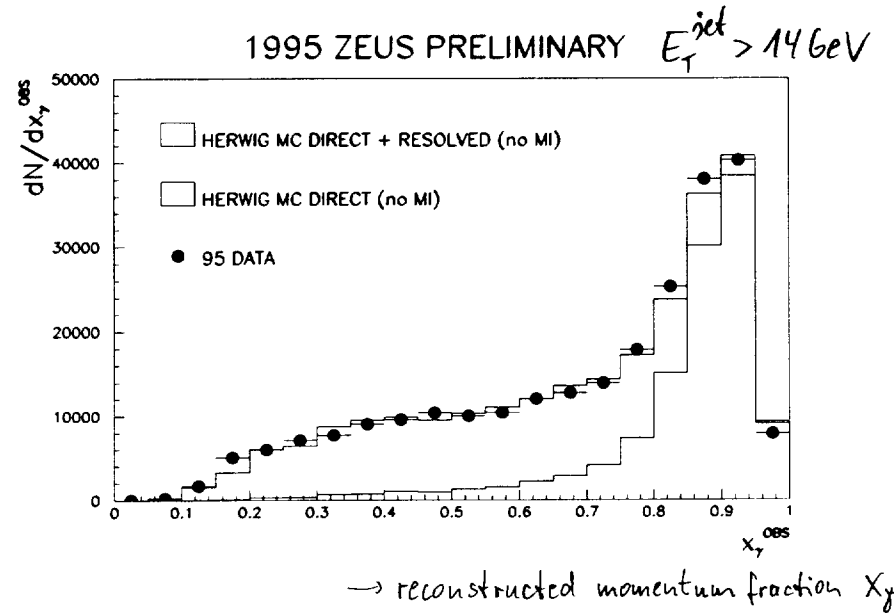
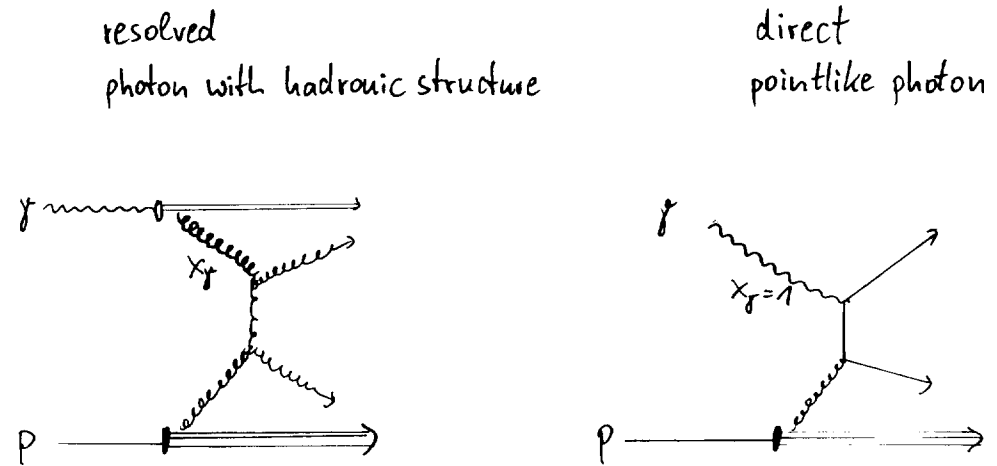
$$\cos \theta^* = \tanh \frac{\Delta \eta_{\text{jets}}}{2} \quad x_p = \frac{1}{2E_p} \sum_{\text{jets}} (E + p_z)$$

4 fold differential di-jet cross section:

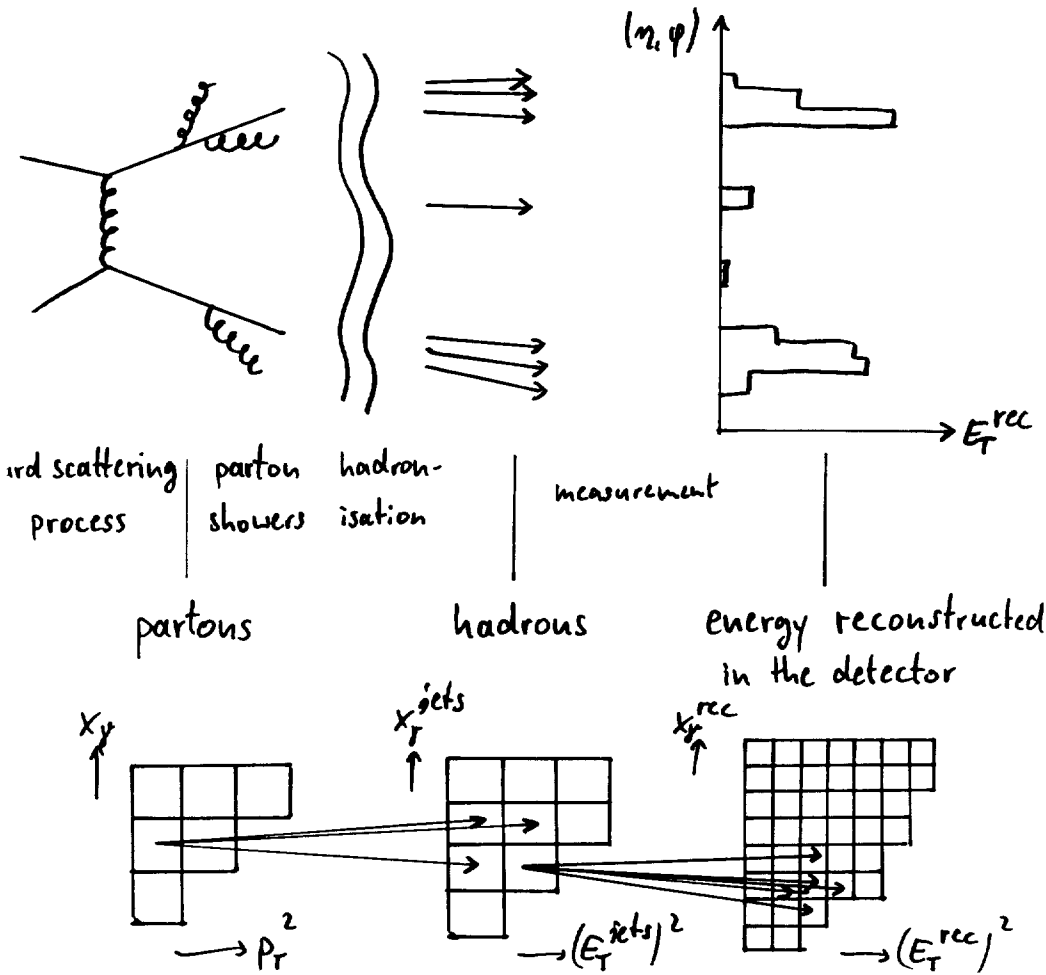
$$\frac{d^4 \sigma}{dy dx_y dx_p d\cos \theta^*} = \frac{1}{32\pi S_{ep}} \frac{f_e(y)}{y} \sum_{i,j} \frac{f_p(x_y, P_T^2)}{x_y} \frac{f_p(x_p, P_T^2)}{x_p} |M_{ij}(\cos \theta^*)|^2$$

transverse momentum of the partons: $P_T^2 = \frac{1}{4} S_{ep} y x_y x_p \sin^2 \theta^*$
with $S_{ep} = (300 \text{ GeV})^2$

Direct and resolved contributions in real photoproduction



Correction of the di-jet cross section



Migrations determined by:

MC model with parton showers and fragmentation

detector simulation

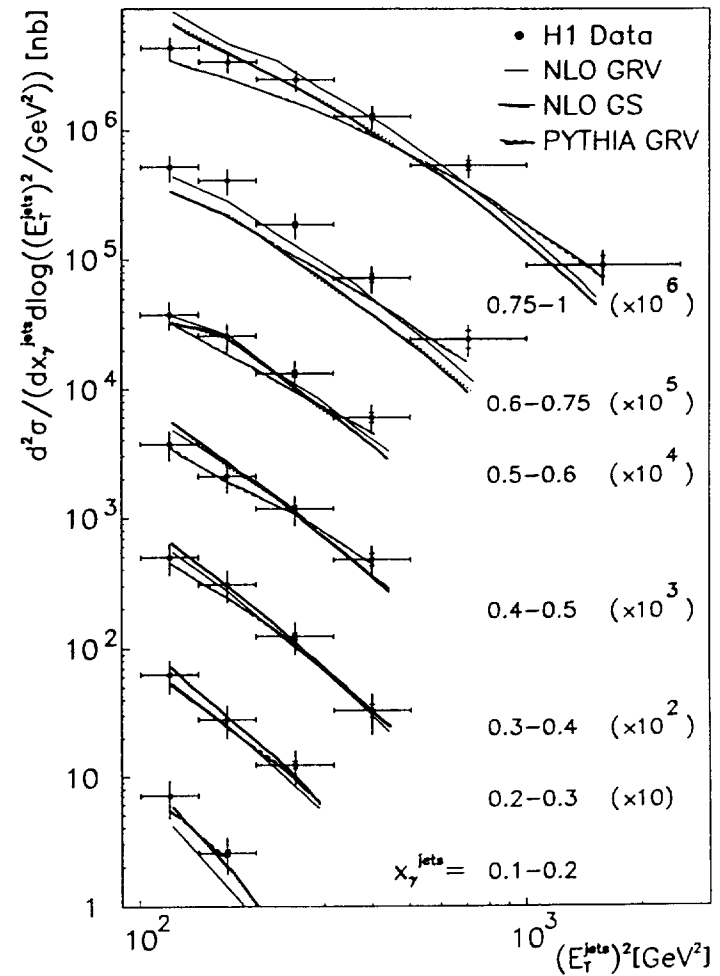
⇒ 2-step unfolding procedure

Inclusive double-differential di-jet cross section

valid for: $Q^2 < 4 \text{ GeV}^2$ $0.2 < y < 0.83$

$$\frac{|E_{T1}^{jet} - E_{T2}^{jet}|}{E_{T1}^{jet} + E_{T2}^{jet}} < \frac{1}{4} \quad 0 < \frac{1}{2}(m_1^{jet} + m_2^{jet}) < 2 \quad |m_1^{jet} - m_2^{jet}| < 1$$

jets defined by cone algorithm, $R=0.7$

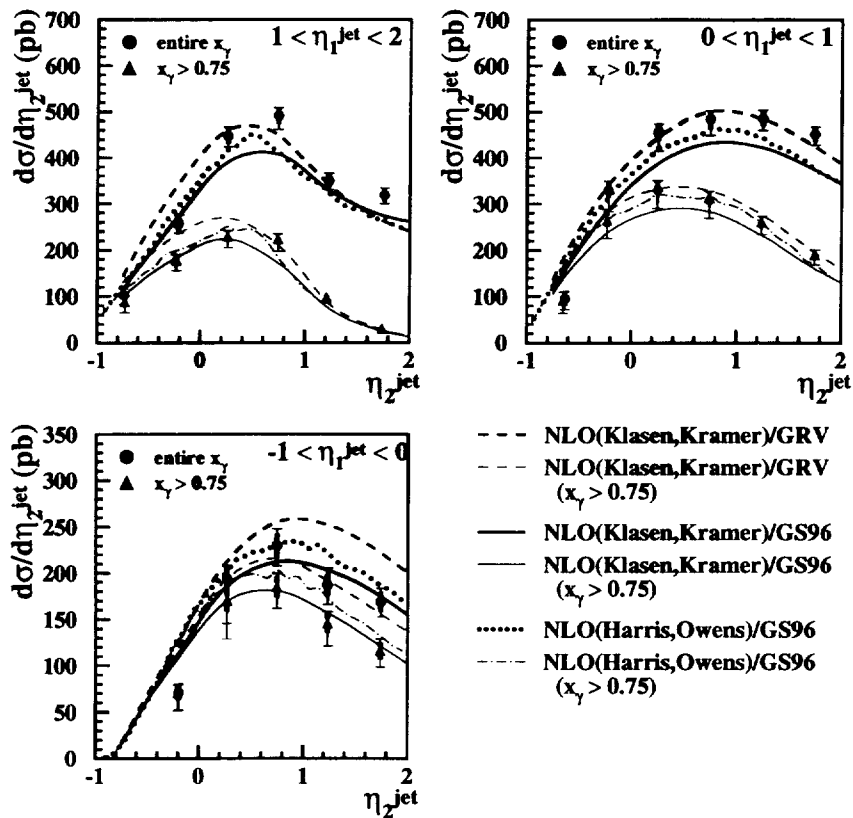


Differential di-jet cross sections

as a function of η_1, η_2, x_γ

$0.2 < y < 0.85, E_T^{\text{jet}} > 14 \text{ GeV}$

ZEUS 1995 preliminary

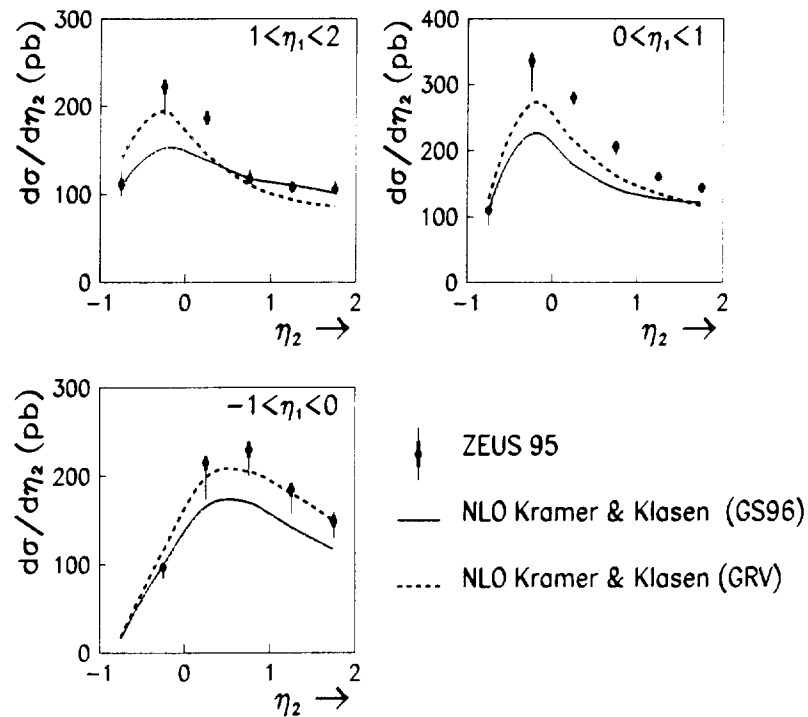


Di-jet cross sections in real photoproduction

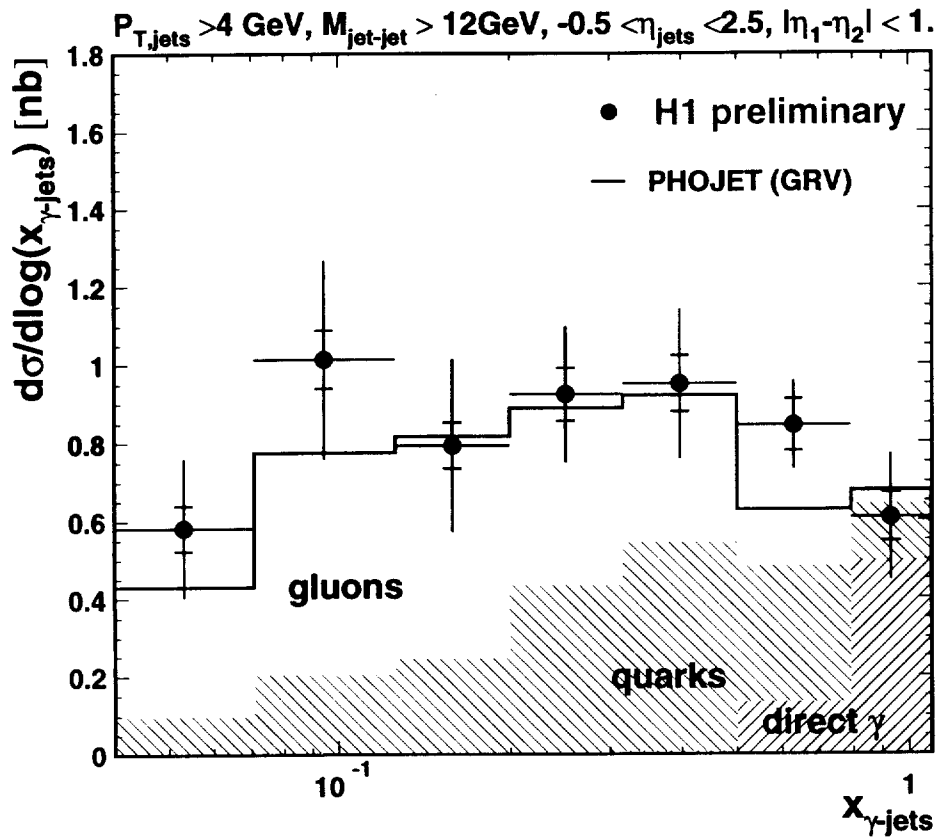
at large center of mass energies:

$0.5 < y < 0.85, E_T^{\text{jet}} > 14 \text{ GeV}$

1995 ZEUS PRELIMINARY



Di-jet cross sections at small x_γ

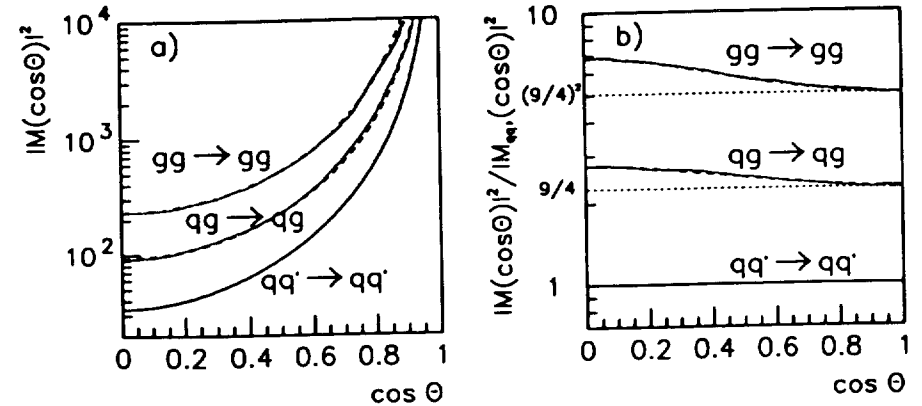


⇒ The contribution from gluons in the photon is essential to describe the observed cross section, especially at small x_γ .

The effective subprocess

Idea (Cambridge/Maxwell 1983):

The angular distributions of the most important partonic scattering processes are similar:



$$|M_{qq' \rightarrow qq'}|^2 : |M_{qg \rightarrow qg}|^2 : |M_{gg \rightarrow gg}|^2 \approx 1 : \frac{9}{4} : \left(\frac{9}{4}\right)^2$$

With the definition of effective parton densities

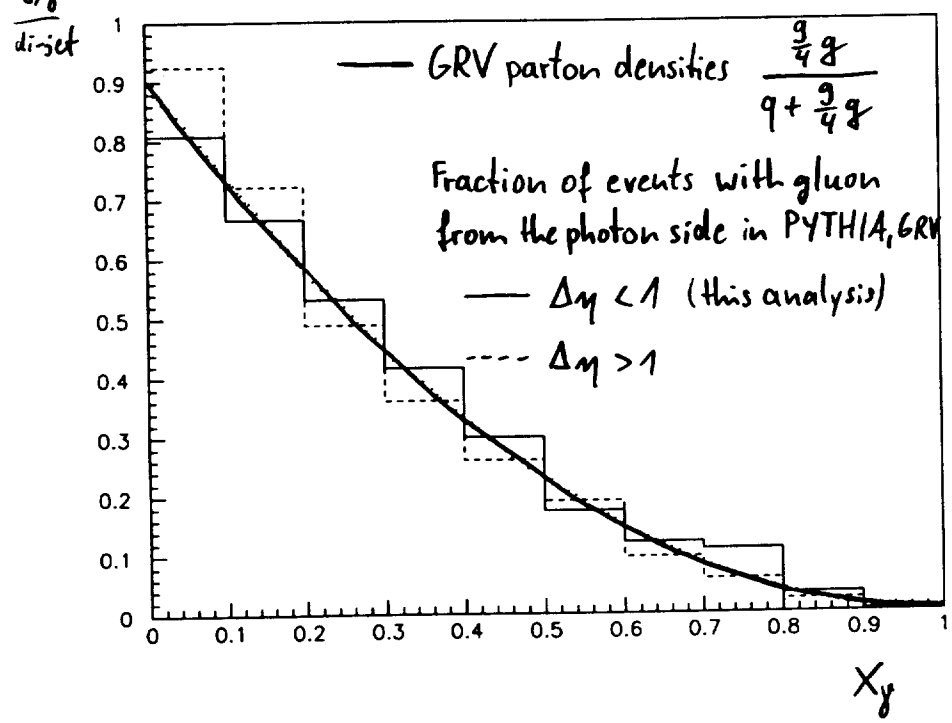
$$f_{eff}(x, p_T^2) = \sum_q (q(x, p_T^2) + \bar{q}(x, p_T^2)) + \frac{9}{4} g(x, p_T^2)$$

the cross section factorizes like a single effective subprocess:

$$\frac{d^4\sigma}{dy dx_\gamma dx_p d\cos\theta^*} = \frac{1}{32\pi s_{ep}} \frac{f(x/e(y))}{Y} \frac{f_{eff}(x_\gamma, p_T^2)}{x_\gamma} \frac{f_{eff}(x_p, p_T^2)}{x_p} |M_{eff}(\cos\theta^*)|^2$$

Precision of the SES approximation

$\frac{g}{g}$ relative gluon contribution to the di-jet cross section



Can we verify the factorisation of the di-jet cross section?

$$\frac{d\delta}{dx_g dx_p} \sim \frac{f_{eff}^g(x_g, p_T^2)}{x_g} \cdot \left(\frac{f_{eff}^p(x_p, p_T^2, x_g)}{x_p} \right)$$

The proton part should be independent of x_g

→ compare x_p -distribution for different x_g bins

however: $x_g^{jets} \sim \frac{p_T}{y} e^{-\bar{\eta}}$

$x_p^{jets} \sim p_T e^{\bar{\eta}}$; $p_T^2 = \frac{1}{4} s_{pp} (y x_g) x_p \sin^2\theta$

We need to keep $y x_g$ constant in order to preserve the shape of the x_p -distribution

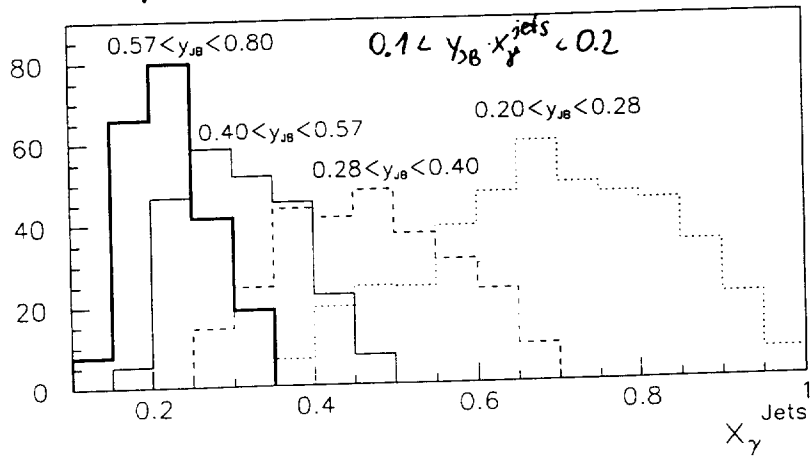
Therefore: fix $0.1 < y_{DB} \cdot x_g^{jets} < 0.2$

and compare x_p for the following (y_{DB}, x_g^{jets}) bins:

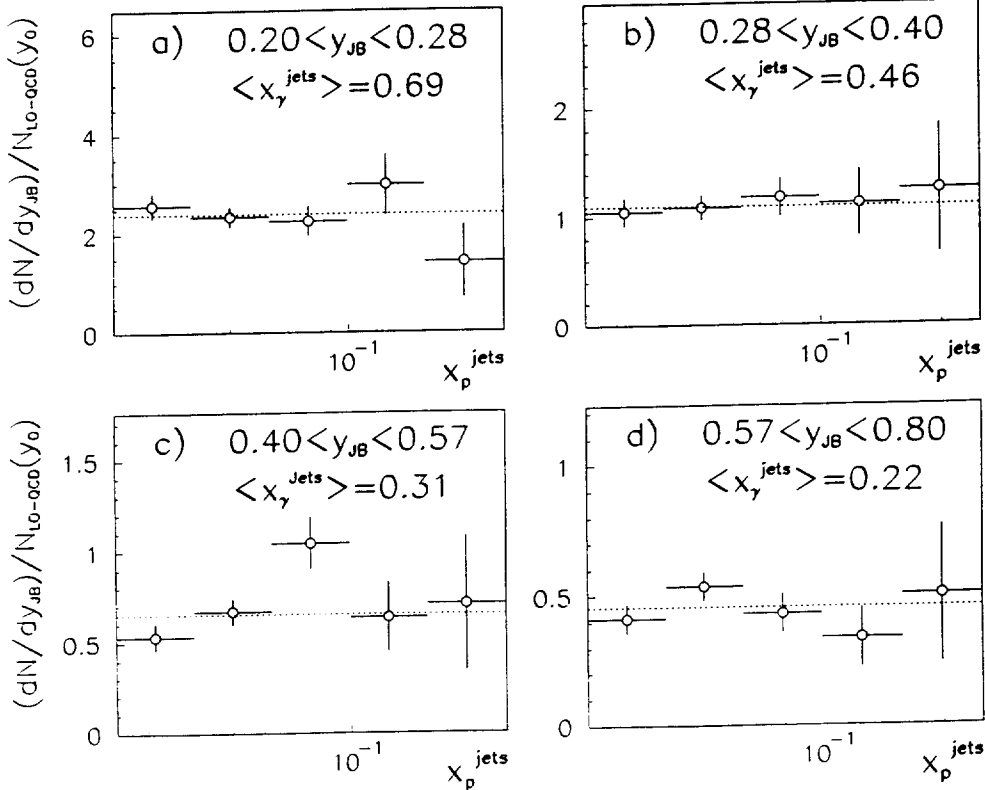
- a) $0.2 < y_{DB} < 0.28$, $0.35 < x_g^{jets} < 1$, $\langle x_p^{jets} \rangle = 0.69$
- b) $0.28 < y_{DB} < 0.4$, $0.25 < x_g^{jets} < 0.7$, $\langle x_p^{jets} \rangle = 0.46$
- c) $0.4 < y_{DB} < 0.57$, $0.18 < x_g^{jets} < 0.5$, $\langle x_p^{jets} \rangle = 0.31$
- d) $0.57 < y_{DB} < 0.8$, $0.12 < x_g^{jets} < 0.35$, $\langle x_p^{jets} \rangle = 0.27$

Factorisation of the di-jet cross section

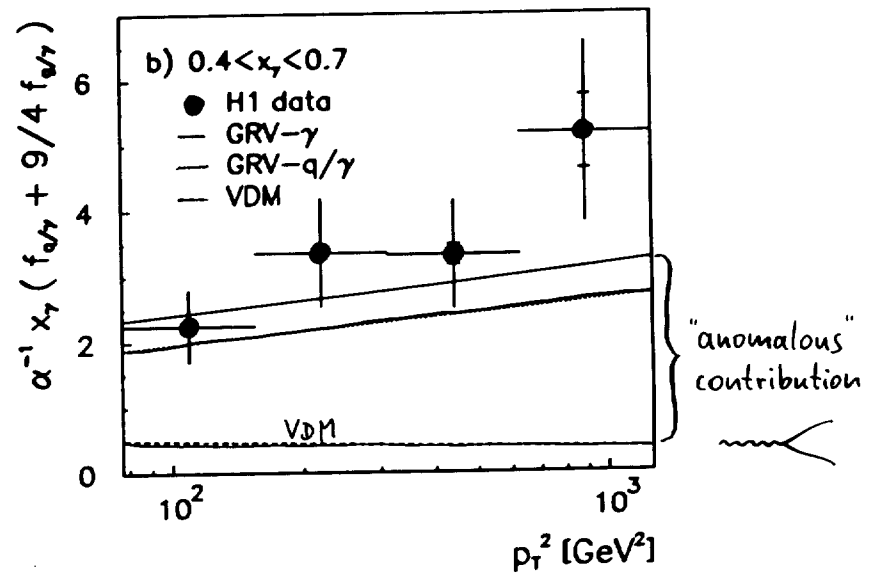
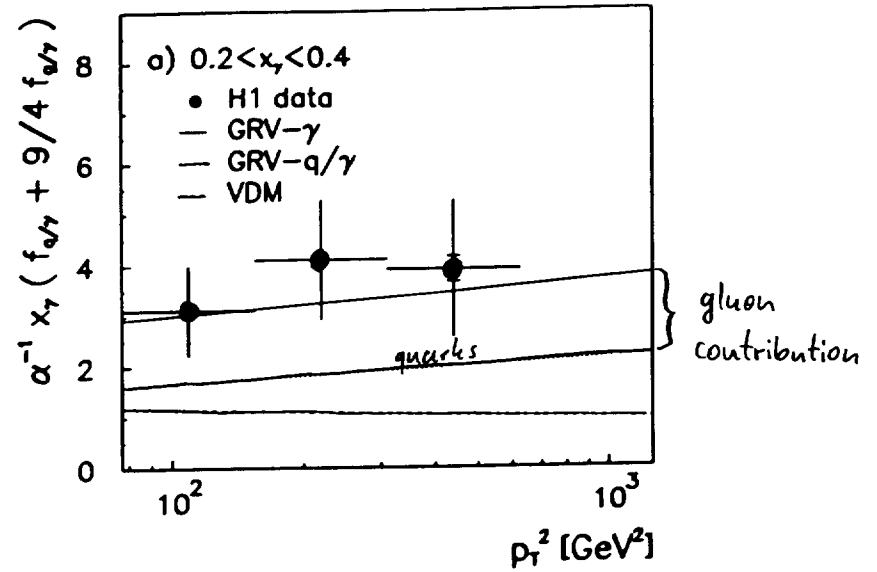
into photon- and proton-dependent parts



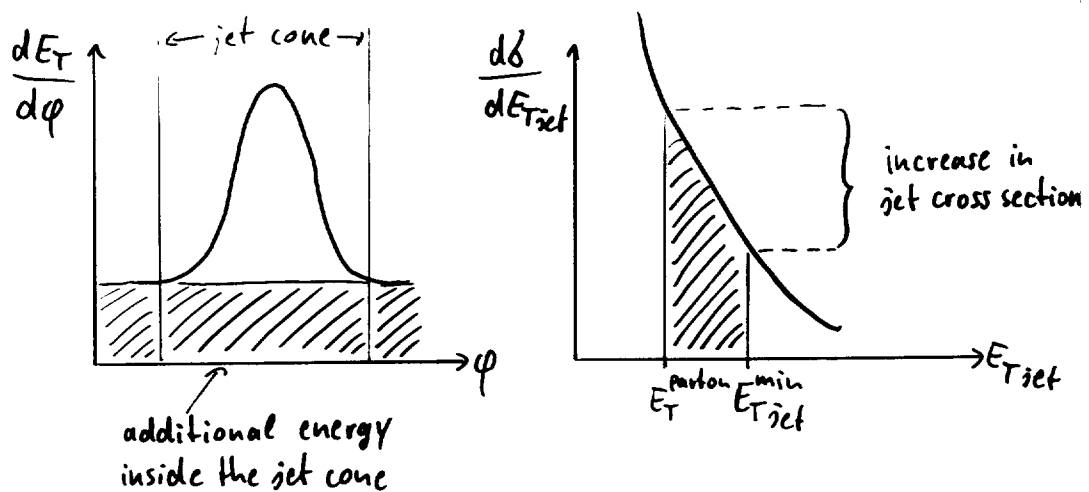
H1 preliminary, uncorrected data



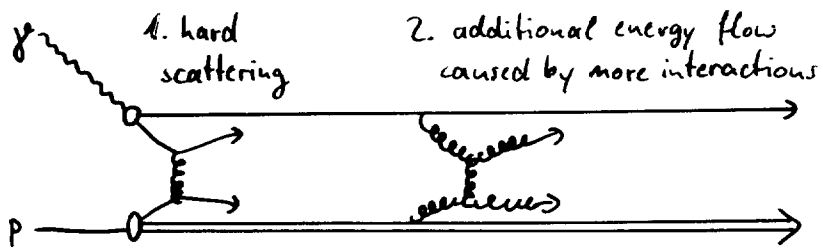
The effective parton distribution of the photon



The energy flow problem



The solution: multiple parton interactions ?

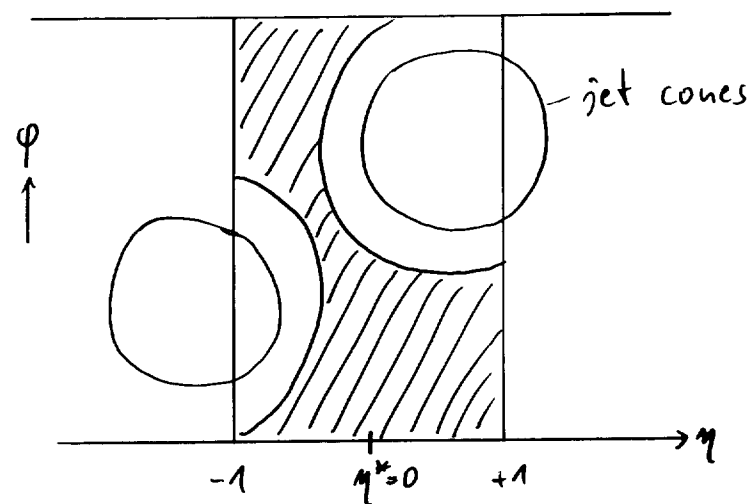


Monte Carlo models

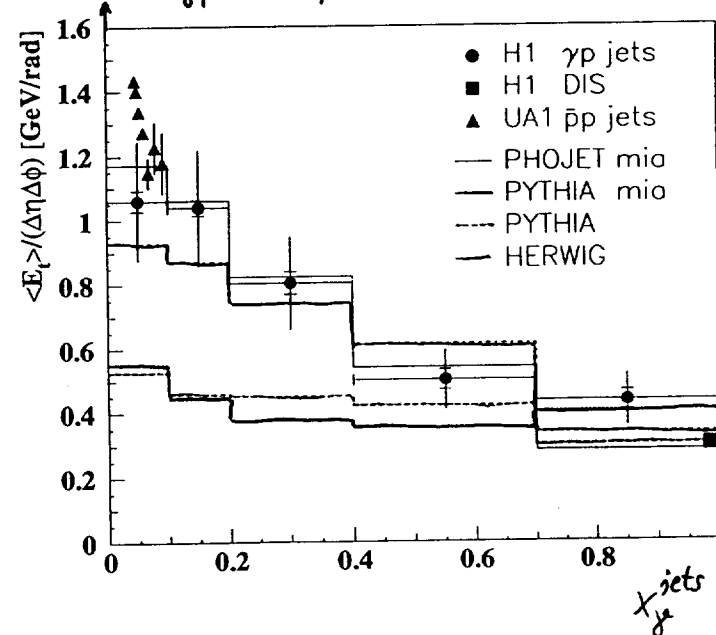
PYTHIA "mia": multiple hard interactions, lower p_T -cutoff for 2nd interaction

PHOJET : smooth transition between soft and hard processes, includes multiple soft and hard interactions

Transverse energy flow outside of jets



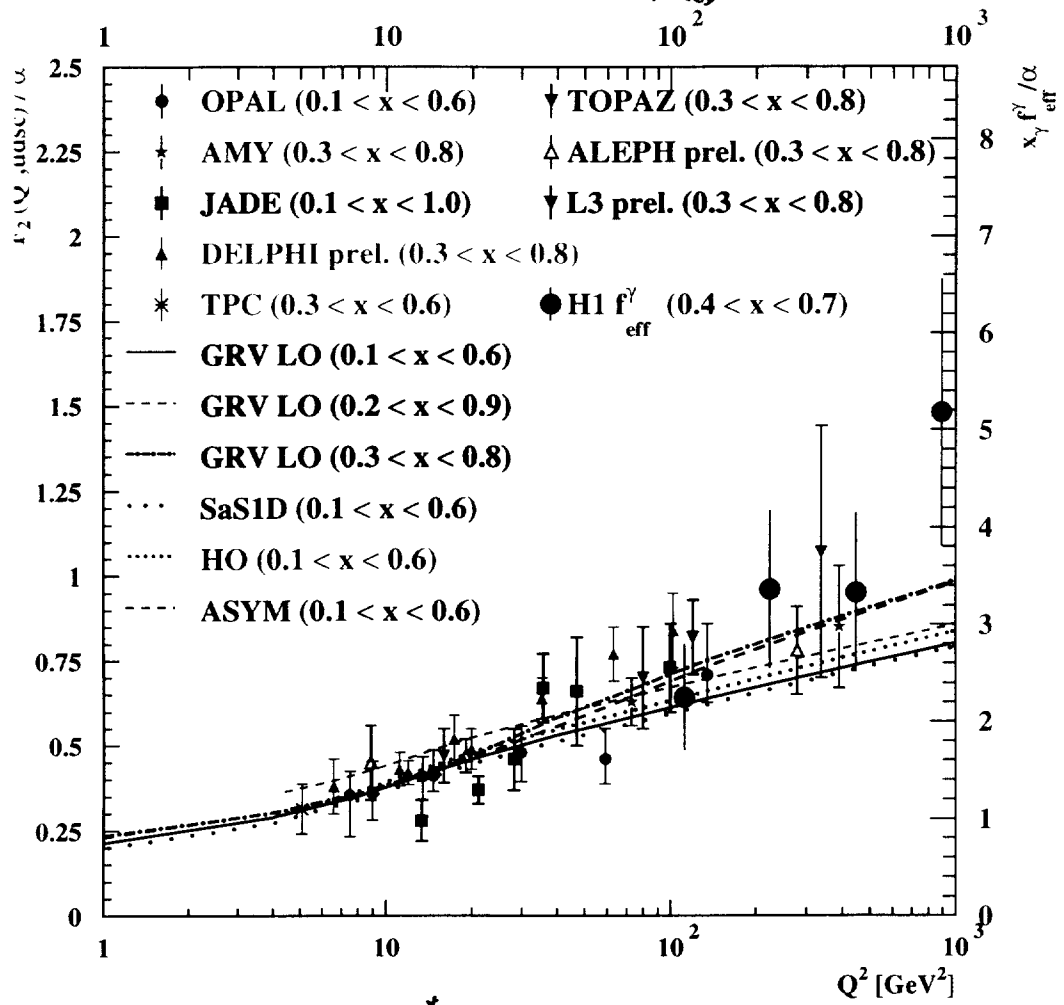
transverse energy density outside of jets



The scale dependence of photon parton distributions

The photon differs from typical hadrons by its electromagnetic coupling to quark pairs:

$$f_{q\gamma}^{QPM}(x_T, p_T^2) \sim (x_T^2 + (1-x_T)^2) \ln \frac{p_T^2}{\Lambda_{QCD}^2}$$



In GRV-LO: $\frac{x_T f_{\gamma}^{eff}}{F_2^{\gamma}} \approx 3.5$

The structure of virtual photons

Classical application of virtual photons:

Deep-inelastic scattering, $Q^2 \gg E_{Tjet}^2$

\Rightarrow pointlike photon probes proton structure, purely 'direct' process

Photoproduction:

$$Q^2 \approx 0$$

\Rightarrow direct pointlike scattering as well as hadronic scattering of the resolved photon

Virtual photon-proton scattering:

$$Q^2 \lesssim E_{Tjet}^2$$

\Rightarrow structure of resolved photon still visible for $Q^2 > 0$

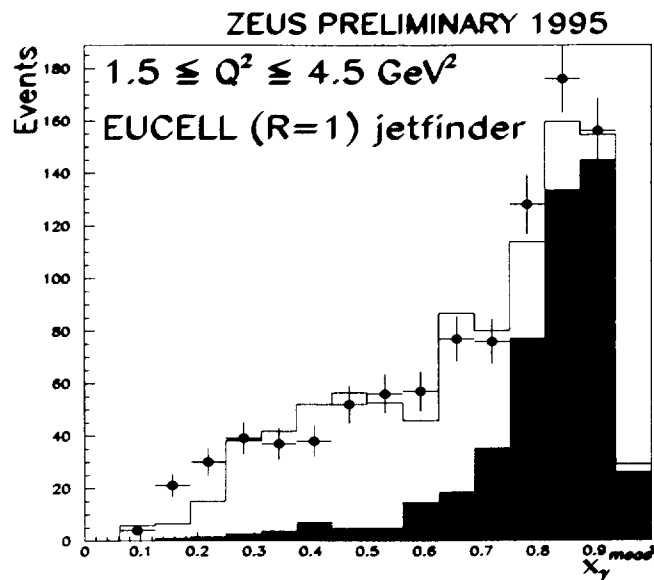
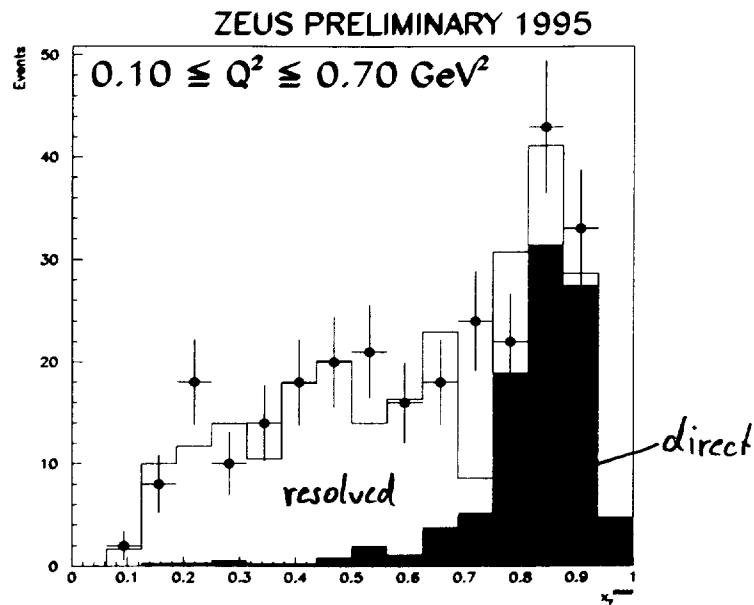
Expect resolved photon contribution to be suppressed with increasing Q^2 , f.ex. Drees-Godbole-Model:

$$\frac{f^{\gamma}(Q^2)}{f^{\gamma}(Q^2=0)} \sim \frac{\ln \frac{p_T^2 + \omega^2}{Q^2 + \omega^2}}{\ln \frac{p_T^2 + \omega^2}{\omega^2}}$$

with free parameter ω

Virtual photon-proton scattering

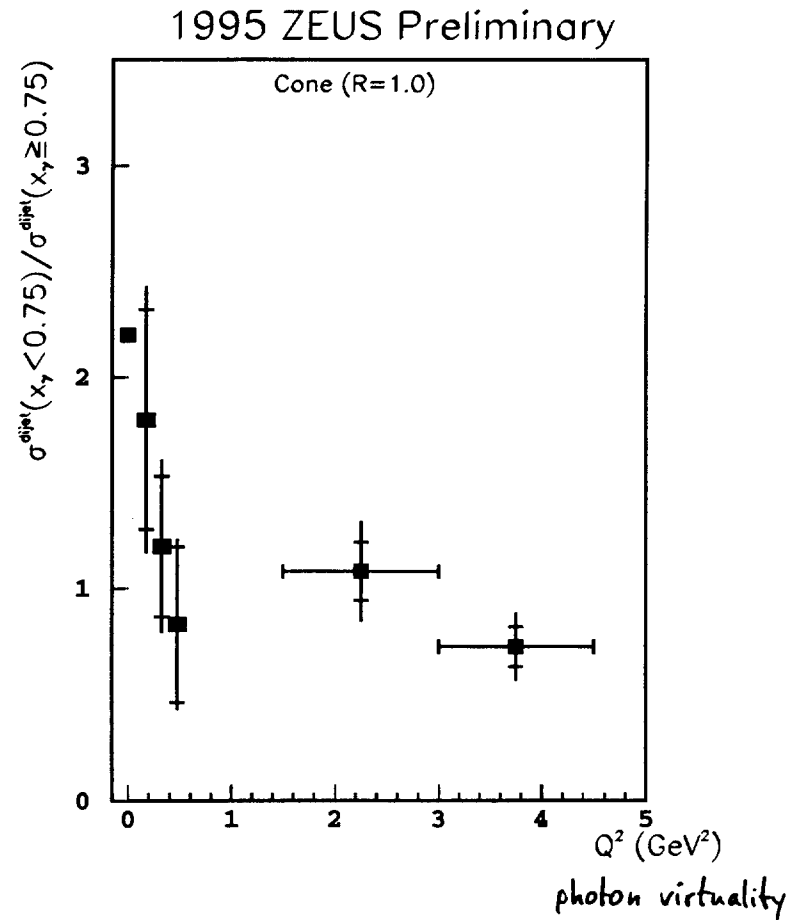
Suppression of the resolved photon component with Q^2



resolved: $x_T^{\text{obs}} < 0.75$

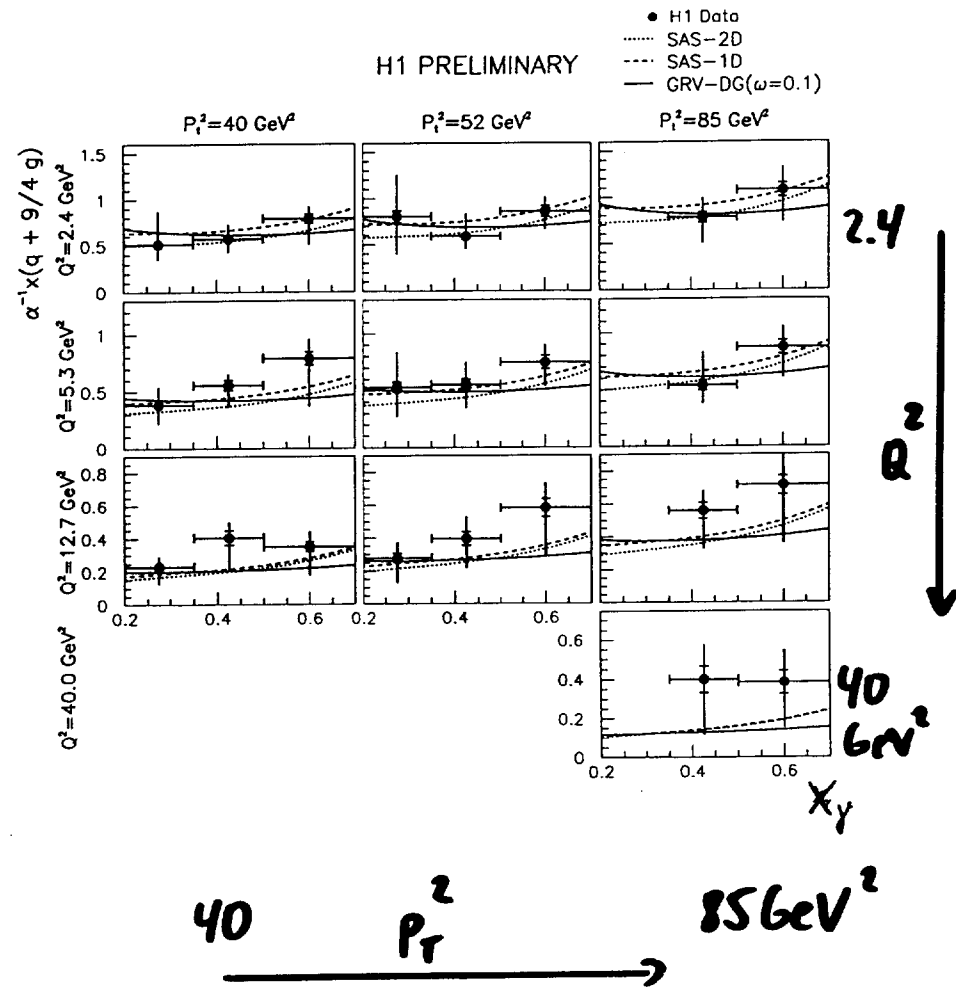
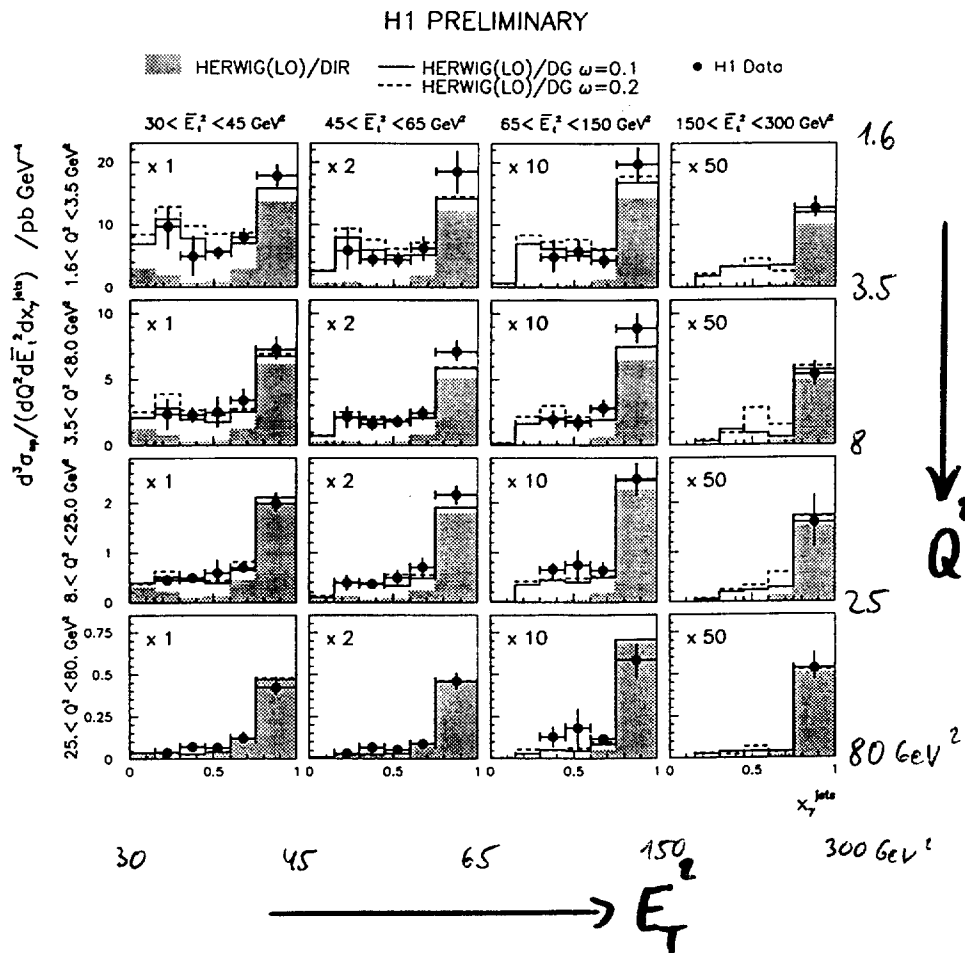
direct: $x_T^{\text{obs}} > 0.75$

ratio
 "resolved"
 "direct"



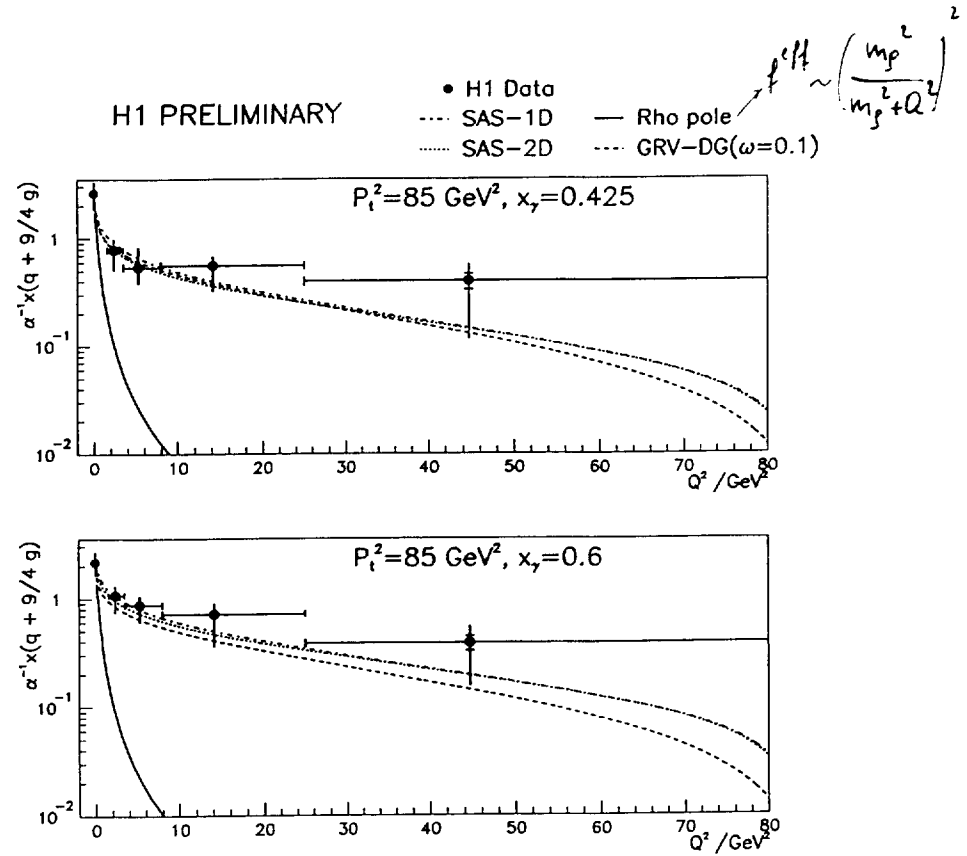
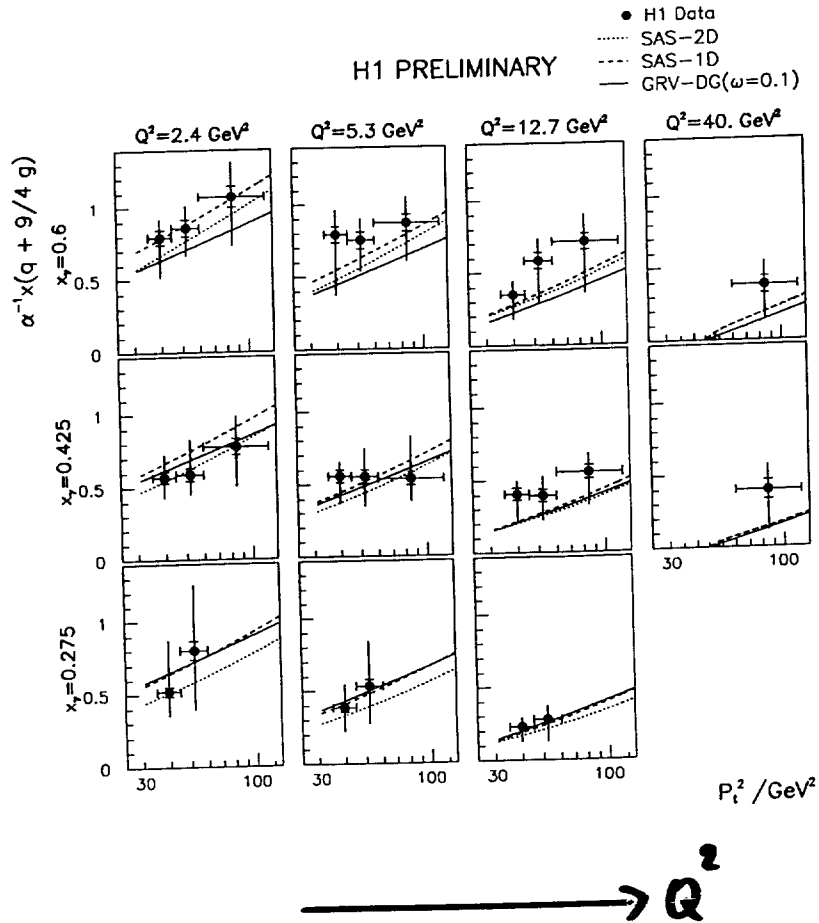
Triple differential di-jet cross section for virtual photon-proton scattering

The effective parton density of the virtual photon



The effective parton density of the virtual photon

Q^2 dependence of the virtual photon parton density



Summary

- * Jet cross section measurements at HERA constrain the parton density of real and virtual photons, complementing and extending photon structure function measurements at e^+e^- experiments.
- * The precision of the data starts to get good enough to distinguish between different parton density parameterizations and to access the gluon content of the photon.
- * The effective parton density of the virtual photon has been measured for the first time.
- * The resolved photon parton density shows the expected scaling behaviour:
 - rising with the scale P_T^2
 - suppressed with increasing virtuality Q^2

